Atmospheric
Chemistry
and Physics
Discussions

Particulate sulfur in the upper troposphere and lowermost stratosphere - sources and climate forcing

Bengt G. Martinsson[1], Johan Friberg[1], Oscar S. Sandvik[1], Markus Hermann[2], Peter F.J. van Velthoven[3] and Andreas Zahn[4]

[1]Division of Nuclear Physics, Lund University, Sweden
[2]Leibniz Institute for Tropospheric Research, Leipzig, Germany
[3]Royal Netherlands Meteorological Institute (KNMI), De Bilt, The Netherlands
[4]Institute of Meteorology and Climate Research, Forschungszentrum Karlsruhe, Karlsruhe, Germany

Correspondence to: B. G. Martinsson (bengt.martinsson@nuclear.lu.se)

Abstract. This study is based on fine mode aerosol samples collected in the upper troposphere (UT) and the lowermost stratosphere (LMS) of the northern hemisphere extratropics during monthly intercontinental flights of the IAGOS-CARIBIC platform in the time period 1999 – 2014. The samples were analyzed for a large number of chemical elements using the accelerator-based methods PIXE (particle-induced X-ray emission) and PESA (particle elastic scattering analysis). Here the particulate sulfur concentrations, obtained by PIXE analysis, are investigated. A steep gradient in particulate sulfur concentration extends several kilometers into the LMS, affected by increasing dilution of particulate sulfur-rich by stratospheric air towards the tropopause. Observed concentrations are related to the distance to the dynamical tropopause. A linear regression methodology revealing seasonal variation and impact from volcanism is used to convert each data point to standalone estimates of a concentration profile and column concentration of particulate sulfur in a 3 km altitude band above the tropopause. We find distinct responses to volcanic eruptions and a significant contribution to the stratospheric aerosol optical depth and radiative forcing of this lowest part of the LMS. Further, the origin of UT particulate sulfur shows a strong seasonal variation. We find that tropospheric sources dominate during summer and fall, whereas these sources make a small contribution during winter and spring. In these latter seasons the stratosphere is the clearly dominating source of particulate sulfur in the UT during moderate volcanic influence as well as background conditions.

1 Introduction

The global mean surface temperature has increased considerably in the two last years (NOAA, Dec. 5, 2016), which followed on a 15-year period with slow temperature evolution. CMIP5 (coupled model intercomparison project) models predict stronger than observed temperature increase in this period (Fyfe et al., 2013; Fyfe et al., 2016). Reasons for these differences were sought, and the Interdecadal Pacific Oscillation connected with increased subduction and upwelling (England et al., 2014; Meehl and Teng, 2014), variations in volcanic aerosol (Solomon et al., 2011; Santer et al., 2014) and solar (Myhre et al., 2013) forcings were identified as main causes of the discrepancies. These phenomena are all elements of natural climate variability, thus highlighting the importance of these influences for assessing the human impact on the climate (Ramanathan and Feng, 2008).

Air from the tropical troposphere containing aerosol precursor gases is lifted into the tropical stratosphere in the Brewer-Dobson circulation. Carbonyl sulfide (OCS) is the most abundant sulfur-containing gas in the atmosphere.

When lofted into the stratosphere, OCS is converted to sulfur dioxide (SO_2) at approximately 25 km altitude aided by UV radiation (Crutzen, 1976) and in a next step to sulfuric acid, giving rise to the background stratospheric aerosol layer. The upward tropical flow is connected with a downward flow in the extratropics, where stratospheric air flows back to the troposphere.

40   The stratospheric aerosol concentration varies strongly due to volcanic influence from events like the strong 1991 Mt. Pinatubo eruption, inducing negative radiative forcing in excess of 1 W/m^2 (McCormick et al., 2005), to close to background conditions at around the turn of the millennium (Bauman et al., 2003; Martinsson et al., 2005). Overall, anthropogenic influence on stratospheric aerosol is small compared to that from volcanism (Neely et al., 2013). Recent volcanic eruptions, such as in 2008 and 2009 of the Kasatochi and Sarychev in the extratropics and in 2011 of the

45   Nabro in the tropics, significantly altered the stratospheric aerosol (Vernier et al., 2011; Bourassa et al., 2012). These eruptions also had a profound impact on the northern hemispheric lowermost stratosphere (LMS) (Martinsson et al., 2009) and the global aerosol optical depth (AOD) of the stratosphere (Andersson et al., 2015). After reaching the LMS, the stratospheric aerosol is transported to the upper troposphere (UT). A recent study indicates that volcanic aerosol also has an indirect climate effect by affecting the reflectance of cirrus clouds in the UT (Friberg et al., 2015).

50   The UT particulate sulfur, in addition, has tropospheric sources. In the tropics, convection lofts aerosol and aerosol precursor gases from low altitudes into the UT (Hess, 2005), whereas in the extratropics both warm conveyor belts (WCB) (Stohl, 2001) and deep convection are the main lofting channels, the latter especially in the summer season. Large amounts of pollutants are long-range transported across the Pacific and Atlantic oceans, where sources are affecting the background concentrations of various species over remote continents. This transport is most efficient

55   above the boundary layer in the pressure interval 700 – 900 hPa (Luan and Jaeglé, 2013). WCBs reaching the UT have their maximum frequency in the winter (Eckhardt et al., 2004) and transport of boundary layer air into the LMS maximizes in the winter and spring (Skerlak et al., 2014), whereas deep convection dominates in the summer (Kiley and Fuelberg, 2006). The time required for vertical transport in WCBs is considerably longer than in deep convective systems, which could be of importance for the vertical transport of short-lived species like SO_2 (TF-HTAP-2010).

60   Aerosol particles in the UT and LMS contain a large fraction of sulfur compounds, mostly sulfates (Dibb et al., 2000, Martinsson et al., 2001, Xu et a., 2001; Kojima et al., 2004). These particles also contain a considerable fraction of carbonaceous aerosol (Murphy et al., 1998; Nguyen et al., 2008; Martinsson et al., 2009), whereof a minor fraction is black carbon (Schwarz et al., 2010; Friberg et al., 2014). In some periods, particularly during spring, crustal particles also are found in this part of the atmosphere (Papaspiropoulos et al., 2002).

65   In this study the concentration of particulate sulfur in the UT and LMS is investigated based on aerosol samples collected from the IAGOS-CARIBIC platform in the time period 1999 – 2014. In this period the UT and LMS aerosol was affected by volcanism from several eruptions as demonstrated in our previous studies based on this data set (Martinsson et al., 2009; Andersson et al., 2013; Friberg et al., 2014; Martinsson et al., 2014; Friberg et al., 2015; Andersson et al., 2015). The IAGOS-CARIBIC aerosol elemental concentration measurements from the LMS are taken

70   in strong concentration gradients that are affected by mixing tropospheric air into the lowest part of the LMS. Each measurement flight results in a small number of samples, being insufficient to reconstruct the gradient. Therefore, we

Atmospheric
Chemistry
and Physics
Discussions

have frequently relied on concurrent IAGOS-CARIBIC measurements, mostly by relating the particulate sulfur measurements to ozone concentrations to express e.g. volcanic influence on the aerosol concentration (Martinsson et al., 2009). Here we present standalone estimates of the stratospheric sulfur aerosol in terms of concentration profiles
75   and column concentrations based on a new method, which is used to study the AOD of the lowest part of northern hemispheric LMS and its radiative forcing. This study also comprises a discussion on the relative importance of stratospheric and the tropospheric sources to the UT of particulate sulfur, seasonal dependences, and different modes of tropospheric transport involved.

2 Methods

80   ### 2.1 Sampling, analysis and classification

This study is based on measurements of particulate sulfur taken from the IAGOS-CARIBIC platform (Brenninkmeijer et al., 2007; www.caribic-atmospheric.com/), where the atmosphere is studied using a modified passenger aircraft from Lufthansa during monthly sets of usually four intercontinental flights. A large number of trace gases and aerosol parameters are measured from that platform during flights in the altitude range 9 – 12 km, including gaseous and
85   condensed water, O_3, CO, NO/NO_y, VOCs, greenhouse gases, halo-carbons, mercury, particle number concentrations, size distributions and elemental concentrations (Brenninkmeijer et al., 2007, Hermann et al., 2003; Schuck et al., 2009; Baker et al., 2010; Oram et al., 2012; Zahn et al., 2012; Martinsson et al., 2014; Dyroff et al., 2015; Slemr et al., 2016; Hermann et al., 2016).

Aerosol sampling from the IAGOS-CARIBIC platform in the time period 1999 – 2014 has resulted in 1198 samples
90   analyzed for aerosol elemental concentrations. The measurements were mainly taken in the northern hemisphere (NH) extratropics and the tropics, while only a small fraction of the samples were taken in the southern hemisphere. Here the focus is on the LMS and UT of the NH. Aerosol particles in the size range 0.08 – 2 µm were collected with a multi-channel impactor with a collection efficiency of 97% ± 4% (Nguyen et al., 2006). The typical time required to collect one sample is 100 minutes. Accelerator-based methods were used to analyze the collected samples with respect to
95   elemental concentrations. Particle-induced X-ray emission (PIXE) was used to analyze the concentration of elements with atomic number larger than 15 (Martinsson et al., 2001). Concentrations of hydrogen, carbon, nitrogen and oxygen were investigated by particle elastic scattering analysis (PESA; Nguyen and Martinsson, 2007). Here the particulate sulfur concentrations are used. The accuracy of the analyses is estimated to 10% and the combined uncertainty in sampling and analysis is estimated to 12%. Further analytical details are found in Martinsson et al. (2014). Finally, in
100   previous publications based on these data the concentrations are given normalized to standard temperature and pressure, which to its nature is a mixing ratio. Here volume concentrations are used in order to facilitate integration over the aerosol column.

The dynamical tropopause (Gettelman et al, 2011) at the potential vorticity (PV) of 1.5 PVU (potential vorticity units; 1 PVU = 10^{-6} K m^2 kg^{-1} s^{-1}) was used to classify samples with respect to tropospheric and stratospheric air. The PV
105   along the flight track was obtained from archived analyses from ECMWF (European centre for medium-range weather forecasts) with a resolution of 1×1 degree in the horizontal and 91 vertical hybrid sigma-pressure model levels. The

Atmospheric
Chemistry
and Physics
Discussions

PV was interpolated linearly in latitude, longitude, log pressure and time to the position of the IAGOS-CARIBIC aircraft.

2.2 Altitude

110   The UT usually holds significantly lower particulate sulfur concentration than the LMS. Combined with bi-directional exchange of tropospheric and stratospheric air across the tropopause, this leads to a gradient of increasing concentration in the LMS from the tropopause. In addition, the concentration of particulate sulfur in the LMS varies due to the influence from volcanism (Martinsson et al., 2009), which has been shown to cause significant radiative forcing (Andersson et al., 2015). In order to study the particulate sulfur gradient in the LMS, fine aerosol elemental

115   concentration measurements from the IAGOS-CARIBIC platform were used in relation to the distance between measurement position and the tropopause (Z):

$$Z = Z_a - Z_{tp} \qquad (1)$$

where Z_a and Z_{tp} are the altitudes of the aircraft and the tropopause. Z_{tp} refer to the dynamical tropopause of 1.5 PVU, which is a low limit to ensure that very little LMS air will be considered as tropospheric. The Z_{tp} was obtained from

120   the ERA-Interim data of ECMWF, whereas the altitude of the aircraft was obtained from pressure measurement which was converted to altitude using the ECMWF data. The position of the tropopause was obtained using the aircraft as the starting position. If that position is in the UT, i.e. has a potential vorticity lower than 1.5 PVU, the tropopause is found by searching upwards in the potential vorticity field. When the aircraft is located in the stratosphere tropopause folds in a small number of cases induce multiple tropopauses in the vertical direction. In order to handle that problem,

125   searches were undertaken both upwards and downwards to find the tropopause closest to the aircraft. That distance is assigned a positive value irrespective of the tropopause is below or above the aircraft, because positive sign indicates stratospheric air.

The study of the aerosol concentration gradient deals primarily with the LMS. The dataset, however, contains observations both in the LMS and the UT and one sample sometimes contains particles from both regions. These

130   concentrations are connected by the exchange across the tropopause. Figure 1 shows the samples that were taken in the UT during the entire sampling time. It is clear that the dependence on the distance from the tropopause is weak or non-existent ($R^2 = 0.02$). Further evaluation (not shown) by normalization to seasonal average concentrations ($R^2 = 0.008$) or to individual groups of concentration data that will be explained below ($R^2 = 0.004$) did not reveal a UT particulate sulfur concentration dependence on the distance from the tropopause. It should be pointed out that the

135   variability in distance to the tropopause is mainly caused by variability in the altitude of the tropopause, because the altitude of the measurement aircraft is fairly constant. This implies that the distance from the tropopause in Fig. 1 does not reflect the measurement altitude, and hence not temperature decrease in relation to the surface of the earth or the degree of cloud processing. The distance to the tropopause for some summer measurements was very large, due to the seasonality of the position of the tropics. Approximately one third of all stratospheric air masses transported across the

140   extratropical tropopause reach the 500 hPa level of the atmosphere, corresponding to approximately 5000 m transport, in 4 – 5 days (Skerlak et al., 2014). This illustrates that the exchange from the stratosphere goes deep in a rather short time. Based on these observations and arguments, the UT particulate sulfur concentration is considered independent

Atmospheric
Chemistry
and Physics
Discussions

of the distance from the tropopause under presented conditions, and thus indicative of the particulate sulfur concentrations of the air mixed into the LMS.

145 The time required to collect one sample was subdivided into ten time intervals where Z was computed along the flight route. For samples taken in the LMS, the sample was represented by the average distance to the tropopause of the ten time intervals. Those time intervals when the sampling was undertaken in the UT, i.e. with $Z < 0$, Z was set to zero. This implies that samples collected entirely in the UT are found at $Z = 0$ in forthcoming graphs. Some of the samples were collected both in the LMS and in the UT. In these cases, the average Z over the ten time intervals of each sample

150 was computed with all UT parts of a sample was set to $Z = 0$. That way all samples could be utilized to study the particulate sulfur concentration in the LMS.

2.3 Methodology to evaluate the S gradient around the tropopause

The particulate sulfur concentration in the LMS will be investigated by linear regression in three steps. To that end we need to consider that the LMS shows a seasonal dependence induced by variability in stratospheric circulation and

155 exchange across the tropopause over the year. Within one season differences between years can be large, mainly due to varying influence from volcanism. Further, the onset of volcanic influence on the particulate sulfur concentration can cause large variability within the season in the same year, and patchiness of young volcanic clouds can further affect the data analysis.

This study was limited to the extratropics of the NH, because the data set contains few measurements taken in the

160 southern hemisphere. Samples taken north of 30° N were used in this study. The highest latitude of sampling was 77° N, and 90% (5% removed each side) of the samples taken in the range 32 - 64° N. Almost all LMS samples (95%) were taken within 3000 m from the tropopause. In terms of altitude, the results of this study therefore can be considered representative of the range 0 – 3000 m above the tropopause.

In order to obtain statistical significance a large number of measurements is needed. To obtain that, seasons of three

165 months were used. Data from one season were grouped with respect to concentration levels of the different years. This means that groups with varying degrees of volcanic activity were formed. Groups typical of "background" conditions were primarily based on data obtained during the 1999 – 2002 period characterized by low volcanic influence on the stratospheric aerosol (Bauman et al., 2003; Deshler et al., 2008) and data from mid-2013 to mid-2014 when the LMS is back to near-background conditions in the NH extratropics, see Table 1 for relevant volcanic eruptions. Another

170 period that we will return to later is mid-2005 to mid-2008 when the stratosphere was affected by the three tropical eruptions in 2005 – 2006 of Manam, Soufriere Hills and Rabaul (Vernier et al., 2009), which also affected the NH LMS (Friberg et al., 2014). There was some variability during these years, implying that not always all of the years were grouped together. They could be grouped with other years, e.g. 2011 and 2013 often had similar concentrations and gradients during the winter and spring seasons. These groups were handled individually in the regression

175 procedures described next, but in a context of the discussion section these groups of "moderate volcanic influence" were averaged to describe the UT aerosol along with the "background" group described above.

The groups were modeled by an initial unweighted linear regression between the particulate sulfur concentration (C_S) and the altitude above the tropopause (Z). This was undertaken for 4 up to 7 groups of data for each season, and a total of 60 regression groups distributed over 12 overlapping seasons were used. This overlapping places each month in the

180   center of a three-month season thus adjusting to smooth seasonal changes in the UTLS. The overlapping also serves the purpose of exchanging data in the regression, which further tests the stability of the results. Some data were excluded from these regressions, which reduced the amount of data from 765 to 694. Of the excluded 71 samples, 60 pertained to periods when fresh volcanism induced strong patchiness in the particulate sulfur concentration. Eleven samples were considered outliers for other reasons, e.g. single samples affected by volcanism during a season or recent

185   up-transport from strongly polluted regions. Thus, for each season (s) and year (y) in total 60 regressions were undertaken:

$$C_S(y, s, Z) = a(y, s)Z + b(y, s) \qquad (2)$$

where a and b varies with season and the strength of the volcanic influence. An example of such a regression is shown in Fig. 2a. Sometimes the regression failed to reflect the tropopause concentrations because of influence from

190   measurements taken at higher altitudes. In order to well represent the tropopause concentration, a method of forcing the offset towards observed concentrations was used. Due to problems with few observations in the UT, the average of observations up to 300 m above the tropopause ($\langle C_{S,Z<300m} \rangle$) were utilized to obtain a first estimate of the concentration at the tropopause. These averages were related to b(y,s) from the regression according to equation 2 in a weighted regression involving all the data groups of a season, with the inverse of the variance in $\langle C_{S,Z<300m} \rangle$ used as

195   weights (see Fig. 2b):

$$b' = c_1 b(y, s) + c_2 \qquad (3a)$$

and the corresponding slope of each data group of the season becomes

$$a' = (\langle C_{S,w} \rangle - b')/\langle Z_w \rangle \qquad (3b)$$

where index w indicates weighted quantities. This estimate of the offset b′ is thus somewhat affected by stratospheric

200   air since measurements up to 300 m above the tropopause were included. To correct the estimate of the offset, in a third step, the average altitude above the tropopause of these samples ($\langle Z \rangle_{Z<300m}$) was used:

$$b'' = b' - a'\langle Z \rangle_{Z<300m} \qquad (4)$$

and the corresponding, corrected slope (a″) was computed in the same way as a′, but based on b″ (eq. 3b).

The S concentration at the tropopause and in the UT, expressed by b in eq. 2, which, by eq. 3 and 4 transforms to b″,

205   is dependent on the stratospheric concentration which is affected by volcanism (Friberg et al., 2015). This is expressed here by:

$$b''(y, s) = C_{S,UT}(y, s) = a''(y, s)k(s) + C_{S,UTtrop}(s) \qquad (5)$$

resulting in the combined equation:

$$C_S(y, s, Z) = a''(y, s)Z + a''(y, s)k(s) + C_{S,UTtrop}(s) \qquad (6)$$

210   where k(s) reflects stratospheric influence on the UT particulate sulfur concentration and $C_{S,UTtrop}(s)$ is the particulate sulfur concentration of tropospheric origin. The k and $C_{S,UTtrop}$ results of a season are obtained in a weighted linear regression of the offset b″ against the slope a″ (from eq. 6) for all the groups of data available from that season. The inverse variances of b″ are used as weights in the regression. Figure 2c shows an example of this regression step for

the months September to November (SON). The groups of data have different slopes (a″) and offsets (b″) caused

215   mainly by volcanism. Should the stratospheric concentration become as low as the UT concentration, a zero slope a″ would be obtained. Therefore we can estimate the fraction of the UT aerosol of tropospheric origin ($C_{S,UTtrop}$) as the offset of the b″ – a″ regression (Fig. 2c). The slope of that regression shows how the offset b″ changes with increased slope a″, hence expressing the sensitivity (k) of the UT concentration to changes in stratospheric concentration. With access to these two parameters, $C_{S,UTtrop}$(s) and k(s), the LMS concentration gradient and tropopause concentration can

220   be estimated based on a single measurement of the particulate sulfur concentration.

3. Results

The linear regression methodology described in the previous section was applied to particulate sulfur concentrations (C_S) as a function of distance from the tropopause (Z) for seasons comprising three months. Data from different years of one season were grouped according to their concentrations, resulting in several groups differing with respect to the

225   C_S – Z relation. The resulting groups of data from each season were modeled by linear regression. These models were, after some further considerations described in section 2, used to model seasonal dependence and the response of the LMS and UT particulate sulfur concentrations to changes induced mainly by volcanic eruptions. An example of the steps in the methodology is shown in Fig. 2.

This methodology was applied to all seasons, having a duration of three months. The final product of the regression

230   methodology of all twelve overlapping seasons is shown in Fig. 3. It is clear that slopes and offsets of the season groups, differing in particulate sulfur concentration related to distance from the tropopause, can readily be described by linear regressions for all twelve three-month seasons. The relation between slopes and offsets has a very strong seasonal dependence. In some seasons small changes in the LMS sulfur concentration slope is connected with a strong change in tropopause sulfur concentration. This is most pronounced for the seasons centered in February, March and

235   April. At the other end, i.e. where changes in the LMS sulfur concentration is connected with small changes in the tropopause concentration, we find the seasons centered in July to November.

The sensitivity of the tropopause and UT concentration to changes in LMS concentration slope is denoted k in equations 5 – 6, which thus is obtained for each regression depicted in Fig. 3. These results are collected in Fig. 4a. The salient features of the seasonal dependence can be described by a Gaussian distribution added to a low, constant

240   background level (Fig. 4a). The maximum sensitivity appears in the late winter and early spring when the upward motion of the tropopause maximizes (Appenzeller et al., 1996). The stratosphere is growing in the fall, i.e. the extratropical tropopause is moving downwards. This delays transport from the stratosphere to the troposphere, which is reflected by a low sensitivity k. This sensitivity can, in addition, be affected by the residence time of particulate sulfur in the UT. Interestingly, the downward transport in association with the Brewer-Dobson circulation from deeper,

245   aerosol-rich stratospheric layers through the LMS takes place in the same season as the maximum in k, thus further enhancing the stratospheric influence on the UT by the term a″(y,s)×k(s) in eq. 6.

The offsets of the regression lines shown in Fig. 3 (when a″ = 0) expresses the case when the stratospheric and tropospheric concentrations are equal, implying that this offset expresses the particulate sulfur concentration of

Atmospheric
Chemistry
and Physics
Discussions

250 tropospheric origin ($C_{S,UTtrop}$) that is mixed into the LMS, see Fig. 4b. Two Gaussian distributions were used as fits to the seasonal variation of $C_{S,UTtrop}$. As for k, the seasonal variation $C_{S,UTtrop}$ is strong. The seasonal variation of $C_{S,UTtrop}$ will be elaborated in the discussion section.

After obtaining $C_{S,UTtrop}$ and k, the data that are needed for conversion of every measurement of the concentration to an estimate of the slope and offset of the LMS concentration are available. Thus, for each individual measurement (i) in the LMS, consisting of the particulate sulfur concentration ($C_{S,i}$) and the altitude above the tropopause (Z_i), the slope

255 and offset of equations 5 and 6 are obtained from:

$$a_i'' = \frac{C_{S,i} - C_{S,UTtrop}(s)}{Z_i + k(s)} \qquad (7)$$

$$b_i'' = a_i'' k(s) + C_{S,UTtrop}(s) \qquad (8)$$

The estimated slopes and offsets are shown in Figs. 5a and b, where the dots are individual measurements and the histogram monthly averages. Here measurements taken at an altitude of less than 50 m above the tropopause are not

260 shown, because they were judged to have too small stratospheric character for an estimate of the concentration slope in the LMS. Both the slope and the tropopause concentration are affected by volcanism, but the response of the slope is much stronger than that of the tropopause concentration, see e.g. the falls of 2008 and 2009 affected by the Kasatochi and Sarychev eruptions.

Observations at various altitudes above the tropopause are difficult to compare, due to the concentration gradient in

265 the LMS. With the estimates of the tropopause concentration and the slope in the particulate sulfur LMS concentration, each measurement becomes an estimate of the total amount of particulate sulfur in the altitude interval investigated by integration of eq. 6:

$$C_{S,col} = \int_0^{3000} \left(a''(y,s)Z + a''(y,s)k(s) + C_{S,UTtrop}(s) \right) dZ \qquad (9)$$

The particulate sulfur column is calculated for altitudes above the tropopause (Z) in the range 0 to 3000 m, the upper

270 limit because too few measurements (5%) were taken above that level. After integrating the column, it is also interesting to estimate the total amount of sulfur-connected aerosol. To that end, it was assumed that the aerosol consists of 75% sulfuric acid and 25% water, which is a commonly used stratospheric composition (Rosen, 1971; Arnold et al., 1998). This means that the total sulfur column was multiplied by a stoichiometric factor of h = 4.084 to obtain the column of the sulfuric acid – water aerosol:

275 $$C_{A,col} = h C_{S,col} \qquad (10)$$

The measurements were taken in the northern hemispheric latitudes higher than 30° with the highest latitude of 77°, with 90% of the data in the latitude range 34 - 65° N and 70% of the data between 41 and 56° N. The northern mid-latitudes sulfur aerosol columns are shown in Fig. 5c as monthly averages with standard errors (the few months with only one measurement available are shown without an error bar). The sulfur aerosol column of the LMS shows large

280 variability primarily caused by volcanism. The lowest columns are found in the period 1999 – 2002, when the volcanic influence on the stratospheric aerosol was small, see Table 1 over relevant volcanic eruptions. The time period mid-2005 to mid-2008 was affected by tropical volcanism (Vernier et al., 2011), which also caused elevated concentrations in the NH LMS (Friberg et al., 2014). The eruptions of the extratropical volcano Kasatochi in August 2008 placed two volcanic clouds in the stratosphere (Andersson et al., 2015), one in the LMS causing strongly elevated aerosol column

Atmospheric
Chemistry
and Physics
Discussions

285   of the LMS that ceased by November the same year, and the other above the LMS. The latter cloud was transported downward, causing a rise of the LMS aerosol column in December 2008. After some influence from several eruptions of the extratropical volcano Redoubt in the spring of 2009, the eruption of Sarychev strongly affected the northern hemispheric stratosphere from the summer of 2009. The eruption of the Icelandic volcano Grimsvötn in May 2011 had a strong and short impact on the northern LMS, which is reflected by a peak in June to July 2011 (Fig. 5c), before the

290   tropical volcano Nabro reached the northern LMS in the early fall of the same year. After that eruption a gradual decrease of the aerosol load can be seen. The concentrations after mid- 2013 approaches those of the period 1999 – 2002, which was close to stratospheric background conditions.

The LMS aerosol contains a significant fraction of carbonaceous aerosol (Martinsson et al., 2009), mainly organic in nature (Friberg et al., 2014), which will add to the aerosol columns of Fig. 5c and affect the refractive index of the

295   particles. However, this work is dealing with the sulfurous fraction, the main fraction of the stratospheric aerosol. To put the results presented in Fig. 5c into perspective, the AOD will be estimated using a simplified aerosol. Thus, the "standard" stratospheric 75% sulfuric acid – 25% water composition, the particle density 1.669 g/cm^3 and the refractive index 1.44 will be used. Furthermore, particle size distribution measurements from IAGOS-CARIBIC have been taken since 2010 (Hermann et al., 2016). The changes of the size distribution induced by the moderate 2011 eruptions of

300   Grimsvötn and Nabro were small (Martinsson et al., 2014), and agree well with previous measurements (Andersson et al., 2015) of the stratospheric background particle size distribution by Jäger and Deshler (2002). Thus, for the estimation of the AOD the latter particle size distribution was used for the entire time period studied. For fixed composition and particle size distribution the AOD is obtained as a fixed relation to aerosol column: $AOD = fC_{A,col}$, where f contains the relations between mass and area/extinction, in this case $f = 3.29 \cdot 10^{-6}$ m^2/µg. Finally, converting

305   the AOD to radiative forcing (RF) using the global average relation (Hansen et al., 2005; Solomon et al., 2011) of:

$$RF = -25 \times AOD; \quad in\ Wm^{-2} \tag{11}$$

to obtain an estimate of the climate influence of the sulfate aerosol of the lower LMS. The peak AOD of the Kasatochi and Sarychev eruptions is approximately 0.007, corresponding to -0.18 W/m^2 in regional radiative forcing of the lowest 3000 meters of the northern hemisphere LMS. Although no detailed comparisons will be made here, we find that the

310   AOD and radiative forcing obtained from the particulate sulfur measurements show similar tendencies as satellite-based measurements (Andersson et al., 2015). The findings presented here also corroborates the findings of Andersson et al. (2015) on the importance of the LMS for the total stratospheric AOD and radiative impact.

4 Discussion

The results presented here are based on measurements in the extratropical UT and the LMS of the NH, where the latter

315   includes the extratropical transition layer (ExTL). Bi-directional exchange across the tropopause affects strong gradients in the ExTL for species having clearly different stratospheric and tropospheric concentrations (Hoor et al., 2002), such as particulate sulfur (Martinsson et al., 2005). In the previous section, the gradient, UT concentration and column amount of particulate sulfur in the ExTL, with its seasonal dependence and the influence from volcanism (Fig. 5), were investigated. In the processing of the data to obtain these results, in particular one feature stands out: the

320   seasonal dependence of the particulate sulfur concentration from tropospheric sources that is mixed into the ExTL
(Fig. 4b). It shows a broad maximum from June to November and a deep minimum in the late winter and early spring
(February to April).

Let us now compare these concentrations in the UT of tropospheric origin ($C_{S,UTtrop}$) with average concentrations of
particulate sulfur in the UT for two cases: "background conditions" dominated by data from mid-1999 to mid-2002
325   and "moderate volcanic influence" dominated by data from mid-2005 to mid-2008, see section 2.3 for details. The
seasonal dependence of these two categories are shown in Fig. 6a together with $C_{S,UTtrop}$. It is clear that, in line with
the findings of Friberg et al. (2015), the UT particulate sulfur concentration is affected by volcanism. In Fig. 6a we see
that the main differences in UT concentrations of the two cases appears from December to June, coinciding with the
main season of transport from aloft into to the LMS and the shrinkage of the LMS due to tropopause upward motion
330   (Appenzeller et al., 1996; Gettelman et al., 2011). In the period July to November we see a small influence from
volcanism on the UT particulate sulfur concentrations by comparing the background and moderate volcanism cases
(Fig. 6a). Comparing these cases to the concentration of particulate sulfur found to be of tropospheric origin it is clear
that there is a strong agreement between all three categories in the late summer and the fall months, whereas differences
are large during the remainder of the year. The particulate sulfur concentration of stratospheric origin can be estimated
335   by subtracting $C_{S,UTtrop}$ from the two cases of UT concentrations. The results are shown in Fig. 6b, where peak
stratospheric influences of just above 6 and almost 12 ng/m^3 are found in the spring, and minimum contributions of
less than 1 ng/m^3 in the fall for the "background" and "moderate volcanism" cases. Summing the observations up (Fig.
6c), a clear seasonal dependence in the fraction of the UT particulate sulfur concentration originating in the stratosphere
was found, from close to 100% in winter/spring to approximately 10% in late summer and fall. On a yearly average
340   the fraction of the UT particulate sulfur that originates in the stratosphere is approximately 50% during background
conditions and 70% during moderate volcanic influence.

We have found some very distinctive characteristics of the particulate sulfur concentration in the UT, with maximum
in the sources of tropospheric origin in the summer and fall. Carbon monoxide (CO) is often used as a tracer of air
pollution. Zbinden et al. (2013) found winter/spring maximum in the CO concentration in the UT of the NH in contrast
345   to the tropospheric component of the UT particulate sulfur. This contrast can, at least in part, be explained by the
oxidizing capacity in the UT, where the summer abundance of the hydroxyl (OH) radical (Bahm and Khalil, 2004)
induces a decline in CO (Bergamaschi et al., 2000; Osman et al., 2016).

The tropospheric source of UT particulate sulfur could be transported from surface sources of either particulate sulfur
or precursor gases, in the latter case primarily sulfur dioxide (SO_2). Warm conveyor belts (WCB) are transporting large
350   amounts of particles and trace gases from East Asia to North America and from the east coast of North America to
Europe (Luan and Jaeglé, 2013). For sulfate, the most common chemical form of particulate sulfur, the concentration
usually shows a rapid decline with altitude in the troposphere (Heald et al., 2011) associated with formation of
precipitation. Cloud processing also tends to strongly reduce SO_2 concentrations with altitude, where the relative
availability of SO_2 and hydrogen peroxide (H_2O_2) is important for the SO_2 lifetime in the cloud. This seems to suggest
355   that transport of SO_2 to the UT could be especially strong in the winter when the H_2O_2 concentrations are low. However,

Atmospheric
Chemistry
and Physics
Discussions

SO$_2$ measurements by the satellite-based instrument MIPAS indicate, consistent with C$_{S,UTtrop}$ described above, a clear UT seasonal variation with low concentrations in December to March and the highest concentrations in June to September (Höpfner et al., 2015). This seemingly contradictory result could possibly be connected with modes of vertical transport. In fall, winter and spring, with maximum in the winter, vertical transport by WCBs from the boundary layer to the UT is strong (Eckhardt et al., 2004), whereas in the summer deep convection is the most important mode (Hess, 2005; Kiley and Fuelberg, 2006). Deep convection provides a rapid route upwards in the atmosphere, favoring transport of short-lived species like SO$_2$ (TF-HTAP-2010; Dickerson et al., 2007).

Fast summertime transport in deep convection provides high concentrations of SO$_2$ in the UT (Höpfner et al., 2015), which together with a rich abundance of radicals (Bahm and Khalil, 2004) for SO$_2$ conversion to sulfuric acid, forms a plausible explanation for the dominance of tropospheric sources in the UT in the summer and fall, whereas tropospheric sources have only a weak impact on the UT particulate sulfur concentration in the winter and spring. In contrast, the stratosphere was found to be a strong source of the UT particulate sulfur in the latter seasons, and the strength of that source is strongly dependent on the degree of volcanic impact on the stratosphere.

5 Conclusions

Particulate sulfur (usually sulfate) in the upper troposphere (UT) and the lowermost stratosphere (LMS) obtained from the IAGOS-CARIBIC platform was investigated at northern midlatitudes in the time period 1999 – 2014, which covers several tropical and extratropical volcanic eruptions. The study is based on the use of linear regression models, where individual measurements in the strong gradient of the extratropical transition layer (ExTL) can be converted to an estimate of the column of particulate sulfur in a 3000 m layer above the dynamical tropopause (here defined at 1.5 potential vorticity units). The obtained time series in particulate sulfur column concentration shows distinct response to extratropical volcanism and delayed elevation of the column concentration following tropical eruptions. Assuming stratospheric background particle size distribution and composition (75% sulfuric acid and 25% water) the AOD and radiative forcing were estimated, e.g. the peak value following the 2009 Sarychev eruptions were estimated to 0.007 and -0.18 W/m^2, respectively. These estimates refer mainly to the ExTL, i.e. lowest part of the LMS, thus highlighting the importance of the lowest part of the stratosphere for the overall climate impact of volcanism.

As a part of this investigation the sources of UT particulate sulfur were explored. A distinct pattern emerges where tropospheric sulfur sources dominate the supply of particulate sulfur to the UT in the summer and fall. This coincides with the highest concentrations of sulfur dioxide and radicals in the UT and the deep convection season, where the rapid vertical transport provides a pool of UT sulfur dioxide which assisted by high radical concentrations form particulate sulfur. In contrast, during winter and spring the tropospheric sources are very weak. Instead, the seasonal transport down from the stratosphere is a strong source of particulate sulfur. Thus, the stratospheric and tropospheric contributions to the UT have strong and opposite seasonal dependences. On annual average the stratospheric contribution to the UT particulate sulfur is estimated to 50% during stratospheric background conditions. During influence from moderate tropical volcanism the stratospheric fraction rises to 70%. The particulate sulfur concentration in the UT is thus to a large degree governed by the stratosphere and volcanism.

Atmospheric
Chemistry
and Physics
Discussions

Data availability

Data are available upon request to the corresponding author.

Competing interests

The authors declare that they have no conflict of interest.

400   **References**

Andersson, S. M., B. G. Martinsson, J. P. Vernier, J. Friberg, C. A. M. Brenninkmeijer, M. Hermann, P. F. J. van Velthoven, and A. Zahn, Significant radiative impact of volcanic aerosol in the lowermost stratosphere, Nat. Commun. 6:7692 doi:10.1038/ncomms8692, 2015.

Andersson S. M., Martinsson B. G., Friberg J., Brenninkmeijer C. A. M., Rauthe-Schöch A., Hermann M., van
405   Velthoven P. J. F. and Zahn A., Composition and evolution of volcanic aerosol from eruptions of Kasatochi, Sarychev and Eyjafjallajökull in 2008 – 2010 based on CARIBIC observations. Atmos. Chem. Phys. 13, 1781-1796, doi:10.5194/acp-13-1781-2013, 2013.

Appenzeller C., J.R. Holton, and K.H. Rosenlof, Seasonal variation of mass transport across the tropopause, J. Geophys. Res., 101, 15071-15078, 1996.

410   Arnold F., J. Curtis, S. Spreng and T. Deshler: Stratospheric aerosol sulfuric acid: First direct in situ measurement using a novel balloon-based mass spectrometer apparatus, J. Atmos. Chem., 30, 3-10, 1998.

Bahm K. and M.A.K. Khalil, A new model of tropospheric hydroxyl radical concentrations, Chemosphere, 54, 143-166, 2004.

Baker, A. K., Slemr F. and Brenninkmeijer C. A. M., Analysis of non-methane hydrocarbons in air samples collected
415   aboard the CARIBIC passenger aircraft, Atmos. Meas. Tech., 3(1), 311-321, 2010.

Bauman J.J., P.B. Russel, M.A. Geller and P. Hamill: A stratospheric aerosol climatology from SAGE II and CLAES measurements: 2. Results and comparisons, 1984-1999, J. Geophys. Res., 108(D13), 4383, doi:10.1029/2002JD002993, 2003.

Bergamaschi P., R. Heim, M. Heimann and P.J, Crutzen, Inverse modeling of the global CO cycle 1. Inversion of
420   CO mixing ratios, J. Geophys. Res., 105, 1909-1927, 2000.

Atmospheric
Chemistry
and Physics
Discussions

Bourassa A. E., A. Robock, W.J. Randel, T. Deshler, L.A. Rieger, N.D. Lloyd, E.J. Llewellyn and D.A. Degenstein, Large volcanic aerosol load in the stratosphere linked to Asian monsoon transport. Science 337, 78-81, 2012.

Brenninkmeijer C. A. M. , Crutzen P. , Boumard F. , Dauer T. , Dix B. , Ebinghaus R. , Filippi D. , Fischer H. , Franke H. , Frieß U. , Heintzenberg J. , Helleis F. , Hermann M. , Kock H. H. , Koeppel C. , Lelieveld J. , Leuenberger M. , Martinsson B. G. , Miemczyk S. , Moret H. P. , Nguyen H. N. , Nyfeler P. , Oram D. , O'Sullivan D. , Penkett S. , Platt U. , Pupek M. , Ramonet M. , Randa B. , Reichelt M. , Rhee T. S. , Rohwer J. , Rosenfeld K. , Scharffe D. , Schlager H. , Schumann U. , Slemr F. , Sprung D. , Stock P. , Thaler R. , Valentino F. , van Velthoven P. , Waibel A. , Wandel A. , Waschitschek K. , Wiedensohler A. , Xueref-Remy I. , Zahn A. , Zech U. and Ziereis H., Civil aircraft for the regular investigation of the atmosphere based on an instrumented container: the new CARIBIC system. Atmos. Chem. Phys. 7, 4953-4976, 2007.

Brühl C., J. Lilievelt, H. Tost, M. Höpfner and N. Glatthor., Stratospheric sulfur and its implications for radiative forcing simulated by the chemistry climate model EMAC, J. Geophys. Res. 120, 2103-2118, doi:10.1002/2014JD022430, 2015.

Carn, S. A., and F. J. Prata, Satellite-based constraints on explosive SO2 release from Soufrière Hills Volcano, Montserrat, *Geophys. Res. Lett., 37*, doi: 10.1029/2010GL044971, 2010.

Clarisse, L., D. Hurtmans, C. Clerbaux, J. Hadji-Lazaro, Y. Ngadi, and P.-F. Coheur, Retrieval of sulphur dioxide from the infrared atmospheric sounding interferometer (IASI), *Atmos. Meas. Tech., 5*(3), doi: 10.5194/amt-5-581-2012, 2012.

Crutzen P.J., The possible importance of CSO for the sulfate layer of the stratosphere. Geophys. Res. Lett. 3, 73-76, 1976.

Deshler T., A review of global stratospheric aerosol: Measurements, importance, life cycle, and local stratospheric aerosol, Atmos. Res., 90, 223-232, 2008.

Dibb J. E., Talbot R. W. and Scheuer E. M., Composition and distribution of aerosols over the North Atlantic during the subsonic assessment ozone and nitrogen oxide experiment (SONEX), J. Geophys. Res., 105, 3709– 3717, doi:10.1029/1999JD900424, 2000.

Dickerson R. R., C. Li, Z. Li, L.T. Marufu, J.W. Stehr, B. McClure, N. Krotkov, H. Chen, P. Wang, X. Xia, X. Ban, F. Gong, J. Yuan and J. Yang, Aircraft observations of dust and pollutants over northeast China: Insight into the meteorological mechanisms of transport, *Journal of Geophys. Res.*, *112*(D24S90), doi:10.1029/2007JD008999, 2007.

Dyroff C., A. Zahn, E. Christner, R. Forbes, A.M. Tompkins and P.F.J. van Velthoven, Comparison of ECMWF analysis and forecast humidity data with CARIBIC upper troposphere and lower stratosphere observations, Q. J. R. Meteorol. Soc. 141:833-844, doi:10.1002/qj.2400, 2015.

Eckhardt S., A. Stohl, H. Wernli, P. James, C. Forster and N. Spichtinger, A 15-year climatology of Warm Conveyor Belts, J. Climate, 17, 218-237, 2004.

England M. H., S. McGregor, P. Spence, G.A. Meehl, A. Timmermann, W. Cai, A.S. Gupta, M.J. McPhaden, A. Purich and A. Santoso, Recent intensification of wind-driven circulation in the Pacific and the ongoing warming hiatus. Nat. Clim. Change 4, 222-227, 2014.

Friberg, J., B. G. Martinsson, S. M. Andersson, C. A. M. Brenninkmeijer, M. Hermann, P. F. J. van Velthoven, and
A. Zahn, Sources of increase in lowermost stratospheric sulphurous and carbonaceous aerosol background
460   concentrations during 1999-2008 derived from CARIBIC flights, *Tellus B, 66, 23428,*
http://dx.doi.org/10.3402/tellusb.v66.23428, 2014.

Friberg J., B.G. Martinsson, M.K. Sporre, S.M. Andersson, C.A.M. Brenninkmeijer, M. Hermann, P.F.J. van
Velthoven and A. Zahn, Influence of volcanic eruptions on midlatitude upper tropospheric aerosol and
consequences for cirrus clouds, Earth and Space Science, 2, doi:10.1002/2015EA000110, 2015.

465   Fyfe J. C., Gillett N. P. & Zwiers F. W. Overestimated global warming over the past 20 years. Nat. Clim. Change 3,
767-769, 2013.

Fyfe J.C., Meehl G.A., England M.H., Mann M.E., Santer B.D., Flato G.M., Hawkins E., Gillett N. P., Xie S.-P.,
Kosaka Y. and Swart N.C., Making sense of the early-2000s warming slowdown. Nat. Clim. Change 6, 224-228,
2016.

470   Gettelman, A., P. Hoor, L. L. Pan, W. J. Randel, M. I. Hegglin, and T. Birner. The extratropical upper troposphere
and lower stratosphere. *Rev. Geophys.* 49, doi: 10.1029/2011RG000355, 2011.

Hansen J, et al., Efficacy of climate forcings, J. Geophys. Res., 110, D18104, doi:10.1029/2005JD005776, 2005.

Haywood, J. M., A. Jones, L. Clarisse, A. Bourassa, J. Barnes, P. Telford, N. Bellouin, O. Boucher, P. Agnew, and C.
Clerbaux, Observations of the eruption of the Sarychev volcano and simulations using the HadGEM2 climate
475   model, *J. Geophys. Res., 115*(D21), doi: 10.1029/2010JD014447, 2010.

Heald C.L. et al., Exploring the vertical profile of atmospheric organic aerosol: comparing 17 aircraft field campaigns
with a global model, Atmos. Chem. Phys., 11, 12673-12696, doi:10.5194/acp-11-12673-2011, 2011.

Hermann M., Heintzenberg J., Wiedensohler A., Zahn A., Heinrich G. and Brenninkmeijer C. A. M., Meridional
distributions of aerosol particle number concentrations in the upper troposphere and lower stratosphere obtained
480   by Civil Aircraft for Regular Investigation of the Atmosphere Based on an Instrument Container (CARIBIC)
flights, J. Geophys. Res., 108(D3), 4114, doi:10.1029/2001JD001077, 2003.

Hermann M., A. Weigelt, D. Assmann, S., Pfeifer, T. Müller, T. Conrath, j. Voigtländer, J. Heintzenberg, A.
Wiedensohler, B.G. Martinsson, T. Deshler, C.A.M Brenninkmeijer and A. Zahn, An optical particle size
spectrometer for aircraft-borne measurements in IAGOS-CARIBIC, Atmos. Meas. Tech. 9, 2179-2194,
485   doi:10.5194/amt-9-2179-2016, 2016.

Hess, P. G., A comparison of two paradigms: The relative global roles of moist convective versus nonconvective
transport, *Journal of Geophysical Research 110*(D20): D20302, 2005.

Hoor P., H. Fischer, L. Lange and J. Lelieveld, Seasonal variations of a mixing layer in the lowermost stratosphere as
identified by the CO-O3 correlation from in situ measurements, J. Geophys. Res., 107,
490   doi:10.1029/2000JD000289, 2002.

Höpfner M., C.D. Boone, B. Funke, N. Glatthor, U. Grabowski, A. Günther, S. Kellmann, M. Kiefer, A. Linden, S.
Lossow, H.C. Pumphrey, W.G. Read, A. Roiger, G. Stiller, H. Schlager, T. von Clarmann and K. Wissmüller,
Sulfur dioxide (SO_2) from MIPAS in the upper troposphere and lower stratosphere 2002-2012, Atmos. Chem.
Phys., 15, 7017-7037, doi:105194/acp-16-7017-2015, 2015.

Atmospheric
Chemistry
and Physics
Discussions

Open Access

495   Jäger H. and T. Deshler, Lidar backscatter to extinction, mass and area conversions for stratospheric aerosols based
          on midlatitude ballonborne size distribution measurements, Geophys. Res., Lett., 29, 1929,
          doi:10.1029/2002GL015609, 2002.

      Kiley, C. M., and H. E. Fuelberg, An examination of summertime cyclone transport processes during
          Intercontinental Chemical Transport Experiment (INTEX-A), *Journal of Geophysical Research*, *111*(D24S06),
500   2006.

      Kojima, T., Buseck P. R., Wilson J. C., Reeves J. M. and Mahoney M. J., Aerosol particles from tropical convective
          systems: Cloud tops and cirrus anvils, J. Geophys. Res., 109, D12201, doi:10.1029/2003JD004504, 2004.

      Luan Y. and L Jaeglé, (2013), Composite study of aerosol export events from East Asia and North America. Atmos.
          Chem. Phys. 13, 1221-1242, doi:10.5194/acp13-1221-2013.

505   Martinsson B. G., Papaspiropoulos G., Heintzenberg J. and Hermann M., Fine mode particulate sulphur in the
          tropopause region from intercontinental commercial flights. Geophys. Res. Lett. 28, 1175 – 1178, 2001.

      Martinsson, B. G., Nguyen H. N., Brenninkmeijer C. A. M., Zahn A., Heintzenberg J., Hermann M., and van
          Velthoven P. F. J., Characteristics and origin of lowermost stratospheric aerosol at northern midlatitudes under
          volcanically quiescent conditions based on CARIBIC observations, J. Geophys. Res., 110, D12201,
510   doi:10.1029/2004JD005644, 2005.

      Martinsson B. G., Brenninkmeijer C. A. M., Carn S. A., Hermann M., Heue K.-P., van Velthoven P. F. J. and Zahn
          A., Influence of the 2008 Kasatochi volcanic eruption on sulfurous and carbonaceous aerosol constituents in the
          lower stratosphere. Geophys. Res. Lett., 36, L12813, doi:10.1029/2009GL038735, 2009.

      Martinsson, B. G., J. Friberg, S. M. Andersson, A. Weigelt, M. Hermann, D. Assmann, J. Voigtländer, C. A. M.
515   Brenninkmeijer, P. J. F. van Velthoven, and A. Zahn (2014), Comparison between CARIBIC aerosol samples
          analysed by accelerator-based methods and optical particle counter measurements, *Atmos. Meas. Tech., 7*, doi:
          10.5194/amt-7-2581-2014.

      McCormick M.P., L.W. Thomason and C.R. Trepte, Atmospheric effects of the Mt Pinatubo eruption. Nature 373,
          399-404, 1995.

520   Meehl, G. A. & Teng, H. CMIP5 multi-model hindcasts for the mid-1970s shift and early 2000s hiatus and
          predictions for 2016–2035. Geophys. Res. Lett. 41, 1711-1716, 2014.

      Murphy, D. M., Thomson D. S. and Mahoney M. J., In situ measurements of organics, meteoritic material, mercury,
          and other elements in aerosols at 5 to 19 kilometers, Science, 282(5394), doi: 10.1126/science.282.5394.1664,
          1998.

525   Myhre, G. et al. Anthropogenic and Natural Radiative Forcing. In: Climate Change 2013: The Physical Science
          Basis. Contribution of Working Group I to the Fifth Assessment Report of the Intergovernmental Panel on
          Climate Change. Cambridge University Press, Cambridge, United Kingdom and New York, NY, USA, 2013.

      Neely III R.R., O.B. Toon, S. Solomon, J.P. Vernier, C. Alvarez, J.M. English, K.H. Rosenlof, M.J. Mills, C.G.
          Bardeen, J.S. Daniel and J.P Thayer, Recent anthropogenic increases in SO2 from Asia have minimal impact on
530   stratospheric aerosol. Geophys. Res. Lett., 40, 999-1004, doi:10.1002/grl.150263, 2013.

Atmospheric
Chemistry
and Physics
Discussions

Nguyen H. N., Gudmundsson A. and Martinsson B. G., Design and calibration of a multi-channel aerosol sampler for studies of the tropopause region from the CARIBIC platform. Aerosol Science and Technology 40, 649-655, 2006.

Nguyen H. N. and Martinsson B. G., Analysis of C, N and O in aerosol collected on an organic backing using internal blank measurements and variable beam size. Nucl. Instr. and Meth. B 264, 96-102, 2007.

Nguyen H. N., Martinsson B. G., Wagner J. B., Carlemalm E., Ebert M., Weinbruch S., Brenninkmeijer C. A. M., Heintzenberg J., Hermann M., Schuck T., van Velthoven P. F. J. and Zahn A., Chemical composition and morphology of individual aerosol particles from a CARIBIC fight at 10 km altitude between 50^0 N and 30^0 S. J. Geophys. Res., 113, D23209, doi:10.1029/2008JD009956, 2008.

NOAA National Centers for Environmental Information, State of the Climate: Global Analysis for October 2016, published online November 2016, retrieved on December 5, 2016 from http://www.ncdc.noaa.gov/sotc/global/201610.

Oram, D. E., Mani F. S., Laube J. C., Newland M. J., Reeves C. E., Sturges W. T., Penkett S. A., Brenninkmeijer C. A. M., Röckmann T. and Fraser P. J., Long-term tropospheric trend of octafluorocyclobutane (c-C4F8 or PFC-318), Atmos. Chem. Phys., 12, doi: 10.5194/acp-12-261-2012, 2012.

Osman M.K., D.W. Tarasick, J. Liu, O. Moeini, V. Thouret, V.E. Fioletov, M. Parrington and P. Nédélec, Carbon monoxide climatology derived from the trajectory mapping of global MOZAIC-IAGOS data, Atmos. Chem. Phys., 16, 10263-10282, doi:10.5194/acp-16-10263-2016, 2016.

Papaspiropoulos G., Martinsson B. G., Zahn A., Brenninkmeijer C. A. M., Hermann M., Heintzenberg J., Fischer H. and van Velthoven P. F. J., Aerosol elemental concentrations in the tropopause region from intercontinental flights with the CARIBIC platform. J. Geophys. Res. *107*(D23), 4671, doi:10.1029/2002JD002344, 2002.

Prata, A. J., and C. Bernardo, Retrieval of volcanic SO_2 column abundance from atmospheric infrared sounder data, *J. Geophys. Res., 112*, doi: 10.1029/2006JD007955, 2007.

Ramanathan V. and Y. Feng, On avoiding dangerous anthropogenic interference with the climate system: formidable chalenges ahead, Proc. Natl. Acad. Sci. USA, 105, 14245-14250, 2008.

Rosen J.M., The boiling point of stratospheric aerosols, J. Appl. Meteorol., 10, 1044-1045, 1971

Santer, B. D. et al. Volcanic contribution to decadal changes in tropospheric temperature. Nat. Geosci. 7, 185-189, 2014.

Schuck T. J., Brenninkmeijer C. A. M., Slemr F., Xueref-Remy I. and Zahn A., Greenhouse gas analysis of air samples collected onboard the CARIBIC passenger aircraft, Atmos. Meas. Tech., 2(2), 449-464, 2009.

Schwarz, J. P., Spackman J. R., Gao R. S., Watts L. A., Stier P., Schulz M., Davis S. M., Wofsy S. C. and Fahey D. W., Global-scale black carbon profiles observed in the remote atmosphere and compared to models, Geophys. Res. Lett., 37, doi: 10.1029/2010GL044372, 2010

Skerlak B., M. Sprenger and H. Wernli, A global climatology of stratosphere-troposphere exchange using the ERA-Interim data set from 1979 to 2011, Atmos. Chem. Phys. 14, 913-937, doi:10.5194/acp-14-913-2014, 2014.

Slemr F., A. Weigelt, R. Ebinghaus, H.H. Kock, J. Bödewadt, C.A.M Brenninkmeijer, A. Rauthe-Schöch, S. Weber, M. Hermann, J. Becker, A. Zahn and B.G. Martinsson, Atmospheric mercury measurements onboard the CARIBIC passenger aircraft, Atmos. Meas. Tech. 9, 2291-2302, doi:10.5194/amt-9-2291-2016, 2016.

Solomon S., Daniel J. S., Neely III R. R., Vernier J. – P., Dutton E. G. and Thomason L. W., The persistently
570   variable "background" stratospheric aerosol layer and global climate change. Science, 333, 866 – 870, 2011.

Stohl A., A 1-year Lagrangian "climatology" of airstreams in the northern hemisphere troposphere and lowermost
       stratosphere, J. Geophys. Res., 106, 7263-7279, 2001

TF-HTAP-2010: Task Force on Hemispheric Transport of Air Pollution: Hemispheric Transport of Air Pollution
       2010, Air Pollut. Stud. 17, edited by: Dentener, F., Keating, T., and Akimoto, H., UNECE, Geneva, Switzerland,
575   available at: http://www.htap.org/, 2010.

Thomas, H. E., I. M. Watson, S. A. Carn, A. J. Prata, and V. J. Realmuto, A comparison of AIRS, MODIS and OMI
       sulphur dioxide retrievals in volcanic clouds, *Geomatics, Natural Hazards and Risk, 2*(3), doi:
       10.1080/19475705.2011.564212, 2011

Vernier, J. P., J. P. Pommereau, A.Garnier, J. Pelon, N. Larsen, J. Niesen, T. Christensen, F. Cairo, L.W. Thomason,
580   T. Leblanc and I.S. McDermid, Tropical stratospheric aerosol layer from CALIPSO lidar observations. *J.
       Geophys. Res.* 114, doi: 10.1029/2009JD011946, 2009.

Vernier, J.-P., L. W. Thomason, J.-P. Pommereau, A.E. Bourassa, J. Pelon, A. Garnier, A. Hauchecorne, L. Blanot,
       C. Trepte, D. Degenstein and, F. Vargas, Major influence of tropical volcanic eruptions on the stratospheric
       aerosol layer during the last decade, Geophys. Res. Lett., 38, L12807, doi:10.1029/2011GL047563, 2011.

585   Xu, L., Okada K., Iwasaka Y., Hara K., Okuhara Y., Tsutsumi Y. and Shi G., The composition of individual aerosol
       particle in the troposphereand stratosphere over Xianghe (39.45_N, 117.0_E), China, Atmos. Environ.,35, 3145–
       3153, doi:10.1016/S1352-2310(00)00532-X, 2001.

Zahn A., J. Weppner, H. Widmann, H. Schlote-Holubek, B. Burger, T. Kühner and H. Franke, A fast and precise
       chemiluminescence ozone detector for eddy flux and airborne application, Atmos. Meas. Tech. 5, 363-375,
590   doi:10.5194/amt-5-363-2012, 2012.

Zbinden R.M., V. Thouret, P. Ricaud, F. Carminati, J.-P. Cammas and P. Nédélec, Climatology of pure tropospheric
       profiles and column contents of ozone and carbon monoxide using MOZAIC in the mid-northern latitudes (24° N
       to 50° N) from 1994 to 2009, Atmos. Chem. Phys., 13, 12363-12388, doi:10.5194/acp-13-12363-2013, 2013.

Atmospheric
Chemistry
and Physics
Discussions

Open Access

EGU

595 **Tables**

Table 1. Most significant volcanic eruptions for the aerosol concentration in the northern hemisphere LMS in the time period studied.

Volcano	Date	Lat./Long.	SO$_2$ (Tg)
Manam	27 Jan 2005	4° S / 145° E	0.1[a]
Soufriere Hills	20 May 2006	17° N / 62° W	0.2[b]
Rabaul	7 Oct 2006	4° S / 152° E	0.2[a]
Jebel at Tair	30 Sep 2007	16° N / 42° E	0.1[c]
Okmok	12 Jul 2008	53° N / 168° W	0.1[c]
Kasatochi	7 Aug 2008	52° N / 176° W	1.7[c]
Redoubt	23 Mar 2009	60° N / 153° W	0.1[d]
Sarychev	12 Jun 2009	48° N / 153° E	1.2[e]
Grimsvötn	21 May 2011	64° N / 17° W	0.4[f]
Nabro	12 Jun 2011	13° N / 42° E	1.5[f]

[a]Prata and Bernardo, 2007

[b]Carn and Prata, 2010

600   [c]Thomas et al., 2011

[d]Brühl et al., 2015
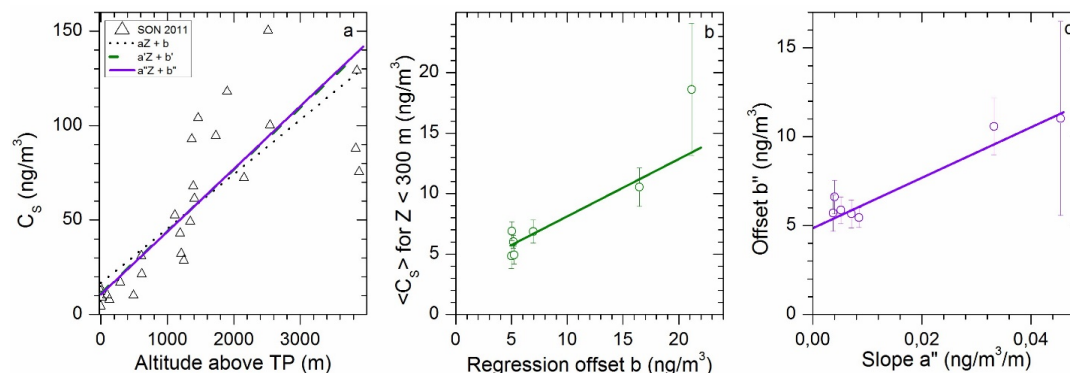
[e]Haywood et al., 2010

[f]Clarisse et al., 2012

Figures

605
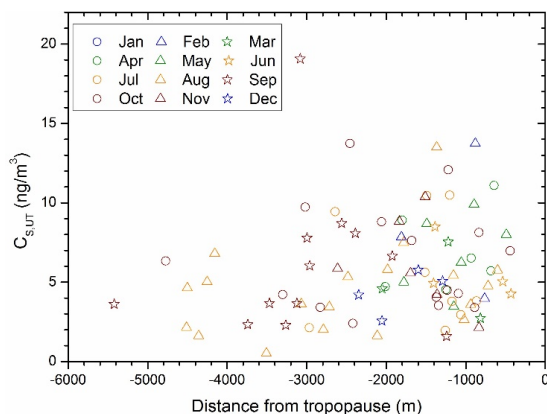
Figure 1: Upper tropospheric particulate sulfur concentration related to distance from the tropopause, where the symbols indicate sampling month.

610 **Figure 2: Example of the regression methodology applied in several steps. (a) Initial linear regression for one group of data taken in September to November (SON) 2011 (black, dotted line). The broken green and purple lines show the change in the regression line induced by forcing the offset and the following correction, see the running text for details. (b) Weighted regression between the offsets from the first regression and the average particulate sulfur concentration in the UT expanded 300 m into the LMS for all SON groups. The group displayed in (a) is found at the x axis value of**

615 **approximately 16 ng/m³. (c) Weighted regression between slopes and offsets of all SON groups. The offset (i.e. when $a'' = 0$) indicates the concentration of tropospheric origin ($C_{S,UTtrop}$) and the slope of the fit (k) expresses the sensitivity of the UT concentration to changes in the stratospheric concentration slope (a''). Denotations a, b, a′, b′, a″ and b″ refer to equations 2 – 6.**
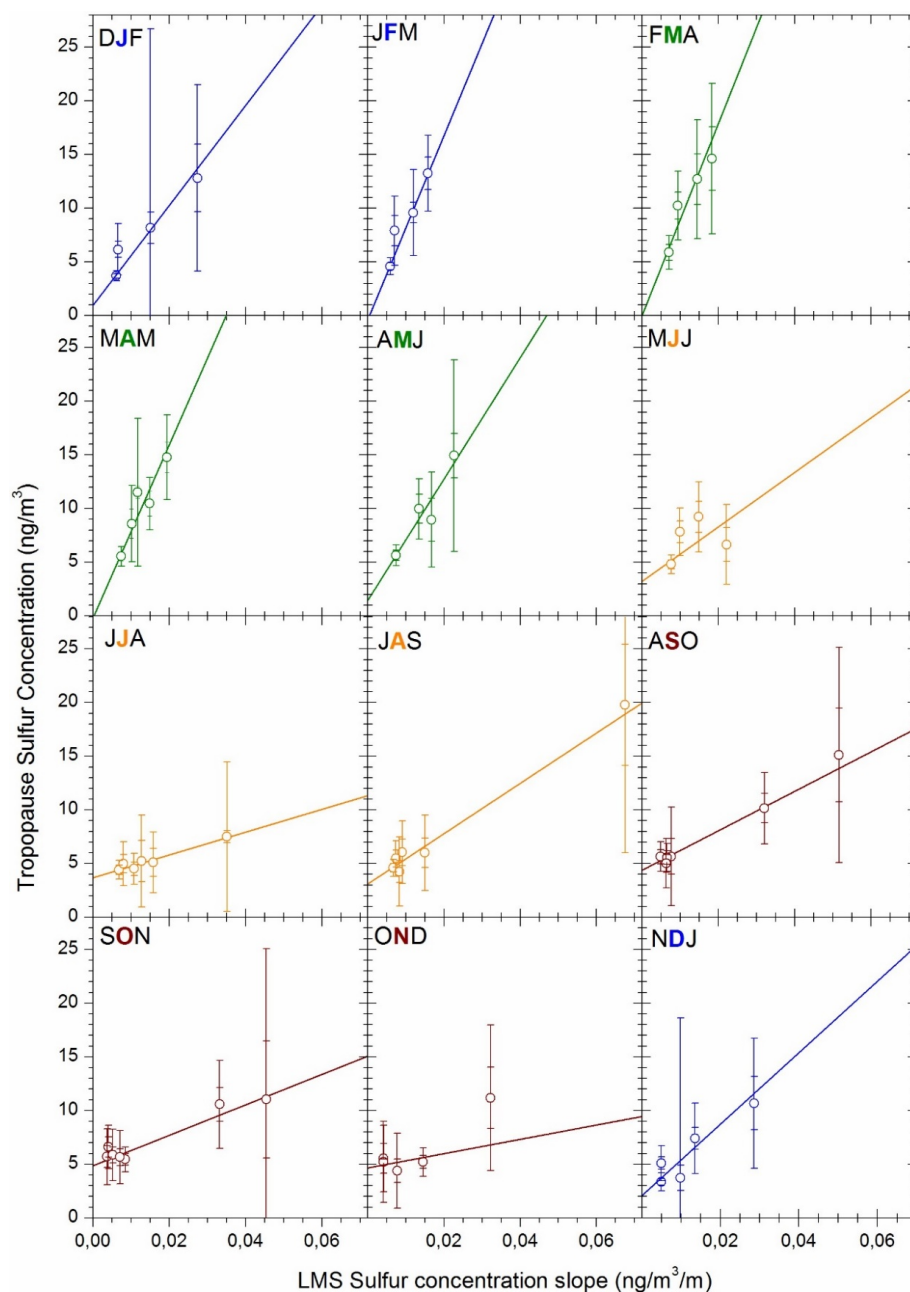
620   Figure 3: Weighted regression between slopes and offsets of all groups of each season (as in Fig. 2c). The offset indicates
the tropopause (and UT) concentration of tropospheric origin ($C_{S,UTtrop}$) and the slope of the fit (k) expresses the sensitivity
of the UT concentration to changes in the stratospheric concentration slope (a''). The error bars show standard deviation
and student-t 95% confidence interval, respectively.
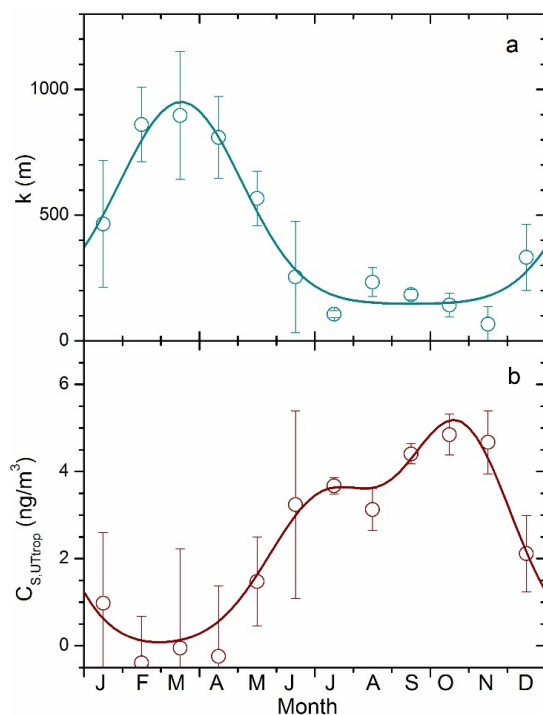
625

Figure 4: Seasonal variation of (a) the sensitivity of the UT aerosol concentration to the concentration slope in the LMS (k), and (b) the UT particulate sulfur concentration of tropospheric origin ($C_{S,UTtrop}$).
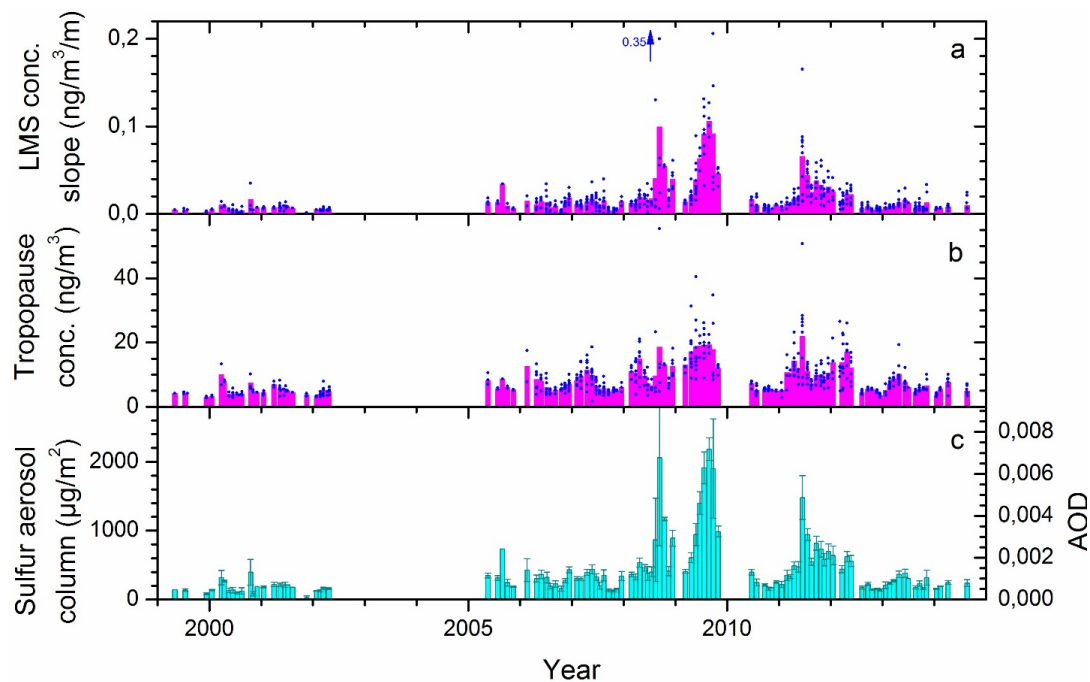
Figure 5: Estimated (a) slopes and (b) offsets based on individual measurements (dots) and monthly averages (magenta bars). (c) Sulfur aerosol column of the lowest 3000 m of the LMS with standard errors, assuming particles of 75% sulfuric acid and 25% water, and AOD (right y axis) assuming stratospheric background aerosol particle size distribution.

630
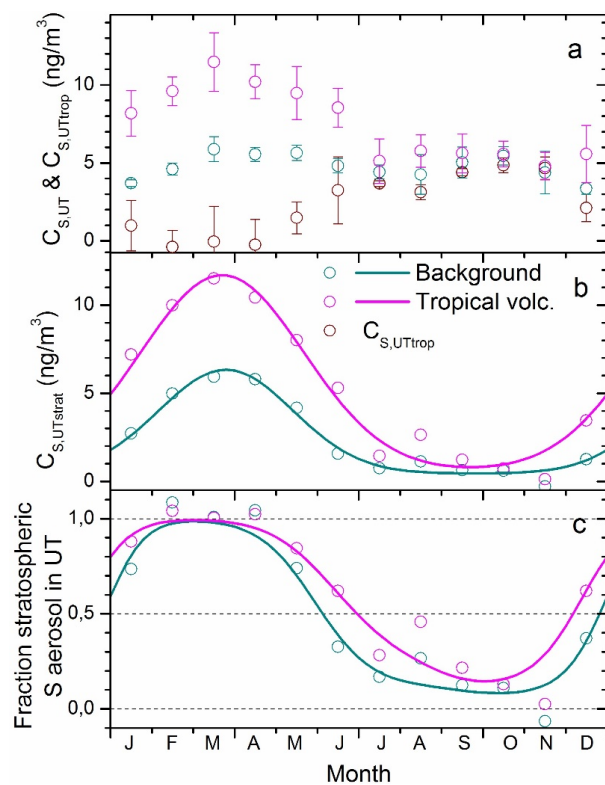
Figure 6. Seasonal variation of (a) the UT particulate sulfur concentration during LMS background conditions and moderate volcanic influence, together with the estimated UT particulate sulfur of tropospheric origin ($C_{S,UTtrop}$), (b) UT particulate sulfur concentration of stratospheric origin ($C_{S,UTstrat}$) obtained by subtracting the $C_{S,UTtrop}$ from the two UT concentration cases in Fig. 6a, and (c) the ratio $C_{S,UTstrat}$ /$C_{S,UT}$ for the two cases.